16th International Conference on Indium Phosphide and Related Materials 2004, 31 May - 4 June, Kagoshima, Japan

MICROELECTROMECHANICAL TUNABLE LONG-WAVELENGTH VERTICAL-CAVITY SEMICONDUCTOR OPTICAL AMPLIFIERS

Garrett D. Cole[1], Qi Chen[2], E. Staffan Björlin[2], Toshio Kimura[2], Shaomin Wu[2], Chad S. Wang[2], John E. Bowers[2], Noel C. MacDonald[1,3]

1) Materials Department, 2) Electrical and Computer Engineering Department, 3) Mechanical Engineering Department, University of California, Santa Barbara, CA 93106, USA
Phone: +1-805-893-5341, Fax: +1-805-893-8486, Email: gcole@engineering.ucsb.edu

Abstract

We present the first demonstration of a microelectromechanical tunable vertical-cavity semiconductor optical amplifier. Electrostatic deflection of the membrane DBR structure has resulted in tunable amplification over an 11-nm wavelength range (1580-1569 nm), with a peak device gain of 17 dB.

I. Introduction

The use of microelectromechanical (MEMS) tuning has become a popular mechanism for wavelength selection in vertical-cavity devices, including vertical-cavity surface-emitting lasers [1-3], resonant-cavity light emitting diodes [4], asymmetric Fabry-Pérot modulators [5], and vertical-cavity filters [6]. In this paper we examine the first MEMS tunable vertical-cavity semiconductor optical amplifier (MT-VCSOA). The device is fabricated using GaAs-based micromachining techniques in conjunction with GaAs to InP wafer bonding in order to fabricate long-wavelength devices containing a tunable air-gap within the structure.

Long-wavelength VCSOAs are attractive devices for use in fiber-optic communication systems. The high finesse Fabry-Pérot (FP) cavity of fixed wavelength VCSOAs results in a narrow gain bandwidth and an inherent filtering effect [7]. This filtering effect is advantageous for preamplifier applications, as it eliminates out-of-band noise and provides channel selection in multi-wavelength systems [8]. In addition, the vertical-cavity geometry of the VCSOA leads to benefits such as high fiber coupling efficiency, polarization independent gain, the potential to fabricate two-dimensional arrays, and the ability to test devices on wafer. In recent years, both optically and electrically-pumped long-wavelength VCSOAs have been demonstrated [7-9].

In order to make VCSOAs more flexible for modern fiber-optic applications, tunable devices must be developed. Previously, temperature tuning of long wavelength VCSOAs has been investigated [10], but a more promising method is MEMS tuning. By integrating a MEMS based electrostatic tuning element with a VCSOA, it is possible to selectively amplify signals over a wider wavelength range. In this case, the FP cavity length is controlled by phase tuning of a suspended distributed Bragg reflector (DBR). Electrostatic force generated by an applied bias results in a deformation of the released structure, reducing the air gap thickness and blue shifting the resonance wavelength. Mechanical alteration of the effective cavity length gives rise to tuning ranges greater than those that can be achieved by refractive index modulation (i.e. temperature tuning).

II. MT-VCSOA design and fabrication

The MT-VCSOA structure consists of an InP-based active region wafer bonded to two AlGaAs DBR mirrors using a direct bonding procedure [11]. The MOCVD-grown active region contains five stacks of five compressively strained AlInGaAs quantum wells placed at the peaks of the standing optical wave in the 5/2-λ cavity, and optimized for optical pumping at 980 nm. The refractive index profile and standing wave pattern of the MT-VCSOA is shown in Figure 1.

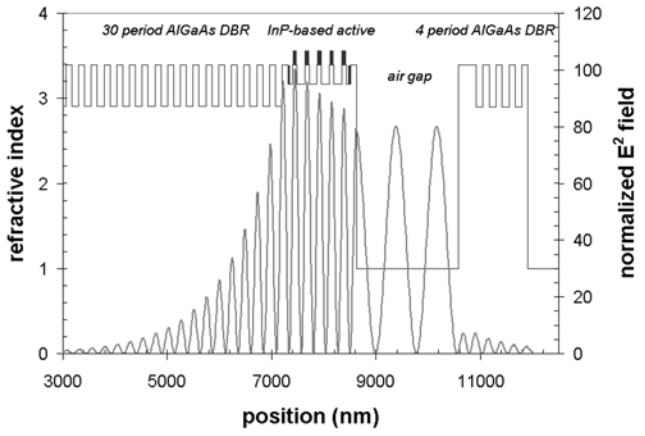

Fig. 1 Standing wave profile for the MT-VCSOA.

For the device presented here, the bottom mirror consists of 30 periods of MBE grown GaAs/$Al_{0.98}Ga_{0.02}As$ resulting in a reflectivity of 0.999. The top mirror structure (from the bottom up) contains a half period of n^+ GaAs, a 5/4-λ (optical thickness in air) $Al_{0.98}Ga_{0.02}As$ sacrificial etch layer (1750-nm intrinsic AlGaAs followed by 200-nm p^+ AlGaAs), a 3/4-λ n^+ GaAs structural layer, and a 4-period GaAs/$Al_{0.98}Ga_{0.02}As$ DBR. The n^+/intrinsic/p^+/n^+ diode forms the MEMS electrostatic tuning structure, allowing for maximum bias with low current. In this case the diode is designed to have a breakdown voltage of 60 V. Following the removal of the sacrificial $Al_{0.98}Ga_{0.02}As$ layer, the air gap, along with the 4 period DBR pillar, forms a 5.5 period DBR including the air gap as a low index layer. The peak reflectivity of this structure is calculated to be 0.976. The MT-VCSOA is designed to be pumped optically, and to operate in reflection mode.

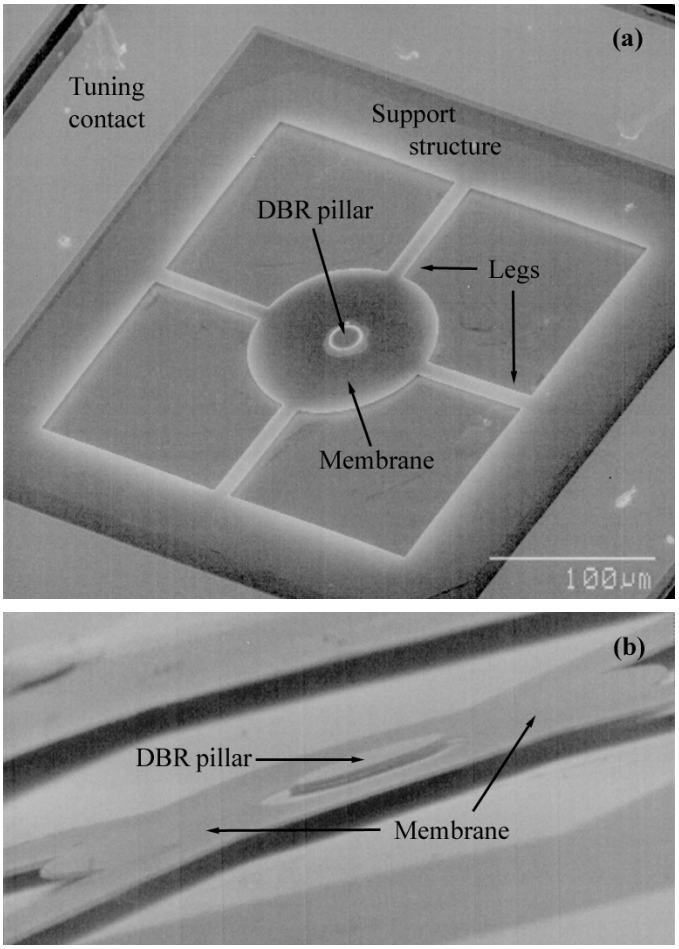

Fig. 2 Scanning-electron micrographs of the MT-VCSOA structure showing (a) overview of a completed device, and (b) a close up of the released membrane.

Following the wafer bonding process, the upper DBR pillar is defined using a chlorine based ($SiCl_4$) dry etch. Next, plasma enhanced chemical vapor deposition is used to deposit a tensile stressed (260 MPa) SiN_x film on the surface of the membrane, which is subsequently patterned to remove the SiN_x from the upper DBR stack. This film is used to create a slight tensile stress in the released membrane, thus ensuring the flatness of the free-standing MEMS structure. Electron beam evaporated Ge/Au/Ni/Au is used to create ohmic contacts to the n^+ GaAs tuning electrodes. In the final step the $Al_{0.98}Ga_{0.02}As$ sacrificial layer is selectively etched in a diluted HCl solution, which laterally undercuts the composite SiN_x/GaAs membrane, leaving an air cavity beneath the structure. When the undercut etch is complete, the structure is placed in a CO_2 critical point drying system in order to avoid collapse of the released membrane. Scanning electron micrographs of a finished device are shown in Figure 2.

III. Device testing and results

The device was pumped from the backside through the GaAs substrate and bottom DBR using a 980-nm laser diode. The MT-VCSOA was operated in reflection mode with the input signal injected through the membrane DBR structure, with the output signal exiting on the same side, as shown in Figure 3. A tunable laser operating near 1550 nm was used as the signal source, while a circulator was used to separate the input and output signals. The total loss through the testing setup was measured to be about 7 dB.

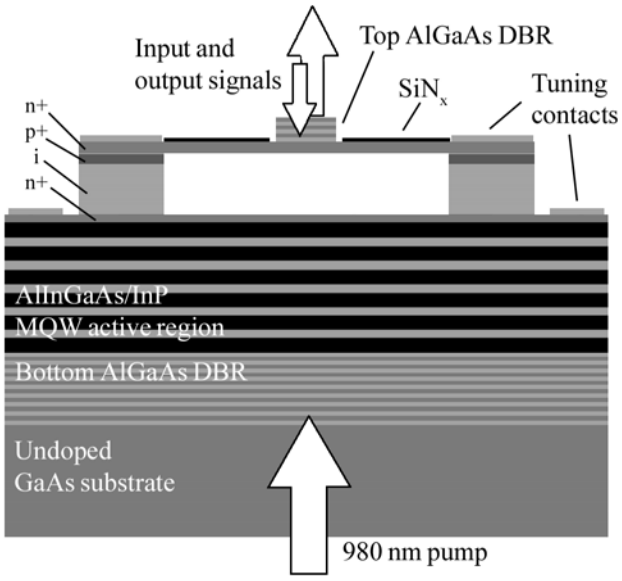

Fig. 3 Reflection mode operation of the MT-VCSOA

Electrostatic tuning of the resonant wavelength is achieved by reverse biasing the n-p-i-n diode structure, resulting in a deflection of the membrane towards the substrate. This deflection reduces the air gap thickness in the upper DBR and results in phase tuning of the top mirror structure, blue shifting the resonant wavelength. Current-voltage testing of the diode structure showed a reverse breakdown voltage of 57 volts.

Following processing, the air-gap thickness is measured using a white light vertical scanning interferometer. In this case the devices show a much larger air-gap than the ideal 5/4-

λ design of 1950 nm. The actual air-gap thickness measured for the device presented here is 3911 nm, due to stress related deformation of the undercut support structure. The dynamic displacement of the released membrane is measured using a laser Doppler vibrometer. With a reverse bias of 57 V, the membrane is displaced by 340 nm. The theoretical and experimental deflection data is presented below in Figure 4. As expected, the deflection shows a parabolic dependence with the applied voltage and the experimental data matches well with the values generated by a one-dimensional electromechanical model similar to that described in [12].

In this device the increase in the air-gap thickness caused by the stress induced support deflection greatly diminishes the applied electrostatic force. With the ideal air-gap, the bias required for 340 nm of displacement would be reduced to 25 V. The deformation of the membrane support material may be alleviated with the addition of a mechanical "clamping" layer, formed by depositing a conformal dielectric film (SiN_x or SiO_2) in order to constrain the support structure and reduce the degree of undesired undercutting [6].

Using the measured deflection data, the resonance wavelength of the device can be calculated. As demonstrated below in Figure 4, the resonant cavity mode blue-shifts from 1590 nm to 1569 nm with a total membrane displacement of 340 nm (tuning bias of 57 V). The measured resonant wavelength follows the theoretical values extremely well; the points of largest error exhibit a red-shift in wavelength due to heating from the high pump power, which is not taken into account in the model.

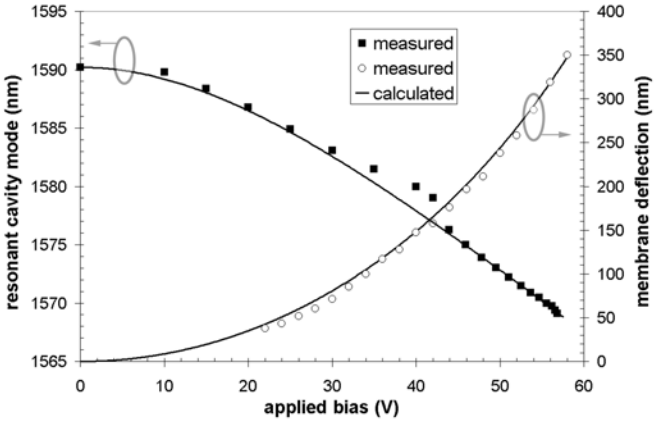

Fig. 4 Wavelength shift and MEMS DBR deflection as a function of the applied tuning bias.

Figure 5 presents the pump power required for 10 dB device gain (3 dB fiber-to-fiber), as well as the calculated mirror reflectance, as a function of wavelength. The reflectance data is generated using an optical simulation program (VERTICAL), while the required pump power is estimated by combining the reflection mode FP gain equation with the carrier rate equation assuming below saturation conditions. As shown in the plot, the MT-VCSOA must be tuned from 1590 nm to 1580 nm before 10 dB of device gain (3 dB fiber-to-fiber gain) is observed.

Device gain larger than 10 dB is measured for wavelengths between 1580 nm and 1569 nm, yielding a tuning range of 11 nm. A maximum device gain of 17 dB (excluding coupling losses) is measured at 1570 nm. As the cavity mode is tuned closer to the QW gain peak less pump power is needed to reach the same gain. In this case the roll-off in material gain at longer wavelengths necessitates higher pump power to achieve the same gain value. In addition to the gain roll-off, the increase in pump power at longer wavelengths is also attributed to insufficient top mirror reflectance.

Over the tuning range the calculated top DBR reflectance varies from 86.8% at the initial cavity mode, to 97.6% near the breakdown voltage of the diode. Because of the non-ideal membrane deflection, the initial air gap results in an optical thickness near a multiple of 1/2-λ. At this point the reflection from the first air-semiconductor interface and the reflection from the bottom of the membrane are nearly out of phase. As the device is tuned, the decreasing air gap thickness begins to approach an odd multiple of 1/4-λ, and the reflected waves begin to add in phase, leading to a large increase in the reflectance of the top mirror structure.

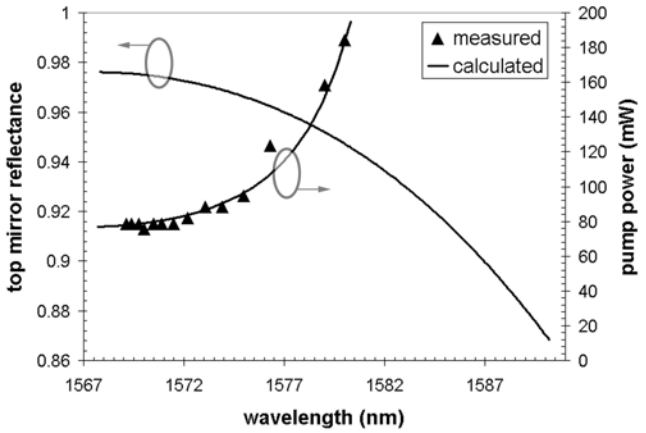

Fig. 5 Experimental and Theoretical top mirror reflectance as well as required pump power for 10 dB device gain as a function of resonance wavelength.

Figure 6 shows the MT-VCSOA gain spectrum at various tuning voltages and pump powers, with an input signal strength of -35 dBm. The solid lines are calculated curve fits based on the FP equations as described in [7] and [10]. As the device is tuned to shorter wavelengths the optical bandwidth decreases, even with the lower pump power shown. This decrease in bandwidth is due to the increased single pass gain at shorter wavelengths arising from both the higher top mirror reflectance (described above), as well as the increased material gain of the active region at the shorter wavelength values. Conversely, at longer wavelengths, the reduced top mirror reflectance coupled with the decreased material gain results in a broadening of the amplifier gain spectrum.

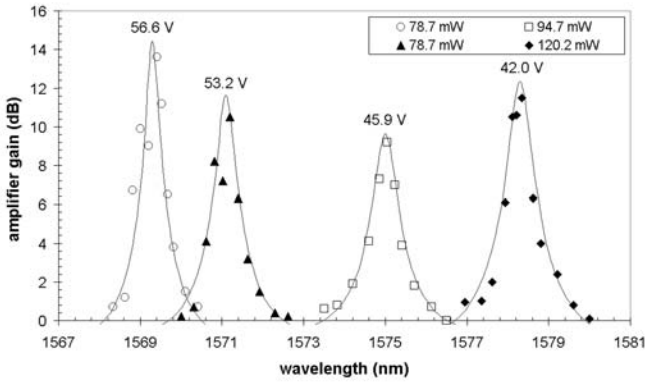

Fig. 6 Amplifier gain spectrum at various tuning voltages.

IV. Summary

A MEMS tunable vertical-cavity semiconductor optical amplifier has been fabricated using a combination of GaAs to InP wafer bonding and GaAs-based micromachining techniques. Completed devices have resulted in a minimum of 10 dB device gain (3 dB of fiber-to-fiber gain) over 11 nm of tuning, with a peak fiber-to-fiber gain of 17 dB (10 dB peak device gain) at 1570 nm.

With an ideal air-gap of 5/4-λ the MT-VCSOA should be capable of tuning ranges exceeding 20 nm, centered at the peak reflectivity of the top DBR structure. In addition, the reduced air gap thickness would allow for much lower tuning voltages. As demonstrated, MT-VCSOAs may be used as channel selective elements in preamplified high bit rate receivers. Additionally, the vertical-cavity structure of a tunable VCSOA allows for the fabrication of 2-D arrays of optical amplifiers, and permits on-chip testing. In this way, arrays of tunable vertical-cavity amplifiers may be fabricated with high yield and low cost.

V. References

1. M. S. Wu, E. C. Vail, G. S. Li, W. Yuen, C. J. Chang-Hasnain, "Tunable micromachined vertical cavity surface emitting laser," *Electronics Letters,* vol. 31, pp. 1671-1672, Sept. 1995.
2. M. C. Larson, A. R. Massengale, J. S. Harris, Jr., "Continuously tunable micromachined vertical-cavity surface-emitting laser with 18 nm wavelength range," *Electronics Letters,* vol. 32, pp. 330-332, Feb. 1996
3. P. Tayebati, P. D. Wang, D. Vakhshoori, C. C. Lu, M. Azimi, R. N. Sacks, "Half-symmetric cavity tunable microelectromechanical VCSEL with single spatial mode," *IEEE Photonics Technology Letters*, vol. 10, pp. 1679-1681, Dec. 1998.
4. G. L. Christensen, A. T. T. D. Tran, Z. H. Zhu, Y. H. Lo, M. Hong, J. P. Mannaerts, R. Bhat, "Long-wavelength resonant vertical-cavity LED/photodetector with a 75-nm tuning range," *IEEE Photonics Technology Letters*, vol. 9, pp. 725-727, June 1997.
5. W. S. Rabinovich, T. H. Stievater, N. A. Papanicolaou, D. S. Katzer, P. G. Goetz, "Demonstration of a microelectromechanical tunable asymmetric Fabry-Perot quantum well modulator," *Applied Physics Letters,* vol. 83, no. 10, pp. 1923-1925, Sept. 2003.
6. J. Daleiden, N. Chitica, M. Strassner, A. Spisser, J. L. Leclercq, P. Viktorovitch, D. Rondi, E. Goutain, J. Peerlings, J. Pfeiffer, R. Reimenschneider, K. Hjort, "Tunable InP/air gap Fabry Perot filter for wavelength division multiplex fiber optical transmission," in *Proceedings of the 11th International Conference on InP and Related Materials*, TuA3-4, pp. 285-287, 16-20 May 1999.
7. J. Piprek, E. S. Björlin, J. E. Bowers, "Optical gain-bandwidth product of vertical cavity laser amplifiers," *Electronics Letters*, vol. 37, pp. 289-299, March 2001.
8. E. S. Björlin, J. Geske, J. E. Bowers, "Optically preamplified receiver at 10 Gb/s using a vertical cavity SOA," *Electronics Letters*, vol. 37, pp. 1474-1475, Nov. 2001.
9. R. Lewen, K. Streubel, A. Karlsson, S. Rapp, "Experimental demonstration of a multifunctional long-wavelength vertical-cavity laser amplifier-detector", *IEEE Photonics Technology Letters*, vol. 10, pp. 1067-1069, Aug. 1998.
10. T. Kimura, E. S. Björlin, J. Piprek, J. E. Bowers, "High-temperature characteristics and tunability of long-wavelength vertical-cavity semiconductor optical amplifiers," *IEEE Photonics Technology Letters,* vol. 15, pp. 1501-1503, Nov. 2003.
11. A. Black, A. R. Hawkins, N. M. Margalit, D. I. Babić, A. L. Holmes, Jr., Y.-L. Chang, P. Abraham, J. E. Bowers, E. L. Hu, "Wafer fusion: materials issues and device results," *IEEE Journal of Selected Topics in Quantum Electronics,* vol. 3, no. 3, pp. 943-951, June 1997.
12. M. C. Larson, "Microelectromechanical wavelength-tunable vertical-cavity light emitters and lasers," Ph.D. dissertation, Stanford University, Stanford, CA, 1996.